Chinese Chemical Letters 34 (2023) 107390

Contents lists available at ScienceDirect

Chinese Chemical Letters

journal homepage: www.elsevier.com/locate/cclet

Ligand-regulated unusual nickel clusters: A centrosymmetric dicubane Ni_8 and a tetrahedral Ni_{10} cluster

Ying Zou[a], Qiang Gao[b], Na Sun[c], Songde Han[a], Xiaoyu Li[a,*], Guoming Wang[a,*]

[a] College of Chemistry and Chemical Engineering, Qingdao University, Qingdao 266071, China
[b] School of Environmental and Chemical Engineering, Jiangsu University of Science and Technology, Zhenjiang 212003, China
[c] The Key Laboratory of Inorganic Molecule-Based Chemistry of Liaoning Province, Shenyang University of Chemical Technology, Shenyang 110142, China

ARTICLE INFO

Article history:
Received 3 March 2022
Revised 27 March 2022
Accepted 30 March 2022
Available online 3 April 2022

Keywords:
Polymetallic
Nickel clusters
Ligand-regulated
Synthesis
Magnetic properties

ABSTRACT

Based on the reported Fe clusters constructed by using *N*-tris(hydroxymethyl)methylglycine (H_5thmmg), herein, we explored the use of H_5thmmg for Ni chemistry. Successfully, an octanuclear Ni cluster, $Ni_8O(H_3thmmg)_6{\cdot}2NO_3$ (**Ni_8**) was acquired under solvothermal condition. Its metallic core is comprised of two centrosymmetric cubanes $Ni_4(\mu_3\text{-}O)_3(\mu_6\text{-}O)$ linked by sharing an O^{2-} ion and six H_3thmmg^{2-} ligands are attached to the periphery. Interestingly, the 2-mercapto-5-amino-1,3,4-thiadiazole (Hmat) ligand with both N and S donor atoms was introduced into the synthesis of **Ni_8** cluster, a disparate decanuclear nickel cluster, $Ni_{10}O(OH)_2(H_3thmmg)_4(mat)_8$ (**Ni_{10}**) is assembled by H_3thmmg^{2-} and mat^- mixed ligands. The metal core of **Ni_{10}** cluster is a pudgy tetrahedron, whose four vertexes are four Ni^{2+} ions and the remanent six Ni^{2+} ions are located in the tetrahedral cavity. Four H_3thmmg^{2-} ligands are located at the four vertices of the tetrahedron and 8 mat^- ligands are all on the six sides of the tetrahedron. The different synthetic conditions contribute to the different configurations. Magnetic studies indicate that both complexes **Ni_8** and **Ni_{10}** display antiferromagnetic interactions.

Owing to the atom-level precise molecular structures and special inorganic polymetallic cores, polynuclear metallic clusters possess the unique physicochemical properties, endowing wide application prospects in the luminescence, photoelectric catalysis, biological imaging, nano-electron and magnetism [1–4]. Now, the fruitful achievement has been gained for noble metal clusters (Cu, Ag, Au) [5–10], polyoxometalates (POMs) [11,12], transition metal clusters [13,14], rare earth metal clusters [15–17], titanium oxide clusters [18] and mixed metal clusters [19–21]. For transition metal clusters chemistry, this new era was triggered by the discovery of the first discrete Mn_{12} molecule with unique single-molecule magnet (SMM) property at the molecular scale [22]. After that, high-nuclearity transition metal clusters with large spin ground electronic states and magnetic anisotropies were pursued to obtain nanoscale excellent SMMs. Mn and Fe clusters have been proven to be two efficient sources of SMMs owing to the molecular anisotropies generated by the Jahn–Teller distortion of Mn(III) and Fe(III) in octahedral coordination geometry [19], exemplified by Mn_{84} [23], Mn_{49} [24], Mn_{30} [25], Mn_{26} [26], Mn_{24} [26], Mn_9 [27], Mn_6 [28], Fe_{19} [29], Fe_{11} [30] and Fe_4 [31]. Besides, V, Cr, Co, Ni and heterometallic 3d-containing transition metal clusters also exhibit the potential capability as the SMMs [20,32–34].

Nickel clusters can be seen as good candidate for SMMs due to their large single-ion zero-field splitting [35,36]. Just like other metal clusters, polynuclear Ni clusters were generally isolated from complex reactive systems influenced by ligand, solvent, pH, temperature, counter-ions and others. An effective synthetic method is to choose polydentate chelate ligands to stabilize supramolecular aggregates of polymetallic ions. Calixarene derivate, polyalcohol acid, pyridine/pyrazolate and oxime have been proven to be prominent species. Liao group adopts the calixarenes derivate to construct a series of various Ni clusters capped different numbers of bowl-like ligands, including Ni_8, Ni_{18}, Ni_{20}, Ni_{24}, Ni_{32} and the largest Ni_{72} cluster [37–39]. By using bi(pyrazole-alcohol) and halogen-substituted pyrazolate, Sun group successfully obtained a Ni_6 with ferromagnetic exchange and three cubic Ni_8 clusters with different magnetic behaviors [40,41]. Furthermore, the pyridine-2-amidoxime and R substituent modification ligands have suitable coordination configurations to construct Ni clusters [42–44]. Based on above ligands, two high-nuclearity Ni_{12} and Ni_{16} with multiple-decker structures were successfully constructed and they display ferromagnetic exchange interactions generating spin ground states

* Corresponding authors.
E-mail addresses: xylichem@126.com (X. Li), gmwang_pub@163.com (G. Wang).

https://doi.org/10.1016/j.cclet.2022.03.113
1001-8417/

of S = 6 for Ni_{12} and S = 8 for Ni_{14} [45]. In addition, by using an achiral citric acid, Güdel group synthesizes a catenulate Ni_{21} with a slow relaxation [33] and two Ni_8 realizing the regulation of magnetic properties by changing the crystallization temperature [46].

Our group recently developed a *N*-tris(hydroxymethyl)methylglycine (H_5thmmg) ligand to synthesize a cyclic Fe_6 cluster and a bricky Fe_{18} cluster seen as a "Chinese knot", providing a potential ligand to construct high-nuclear transition metal clusters [47]. Here, the H_5thmmg ligand was extended to Ni chemistry because of similar coordination configuration of Fe^{3+} and Ni^{2+} ions. Fortunately, an octanuclear Ni cluster has been successfully isolated under solvothermal condition. Its metallic inner is comprised of two centrosymmetric cubanes, $Ni_4(\mu_3\text{-}O)_3(\mu_6\text{-}O)$ by sharing an O^{2-} ion and the periphery is protected by six H_3thmmg^{2-} ligands. In order to regulate the architectures of the Ni clusters, adopting a mixed-ligand strategy, a new 2-mercapto-5-amino-1,3,4-thiadiazole (Hmat) auxiliary ligand with both N and S donor atoms was introduced. As expected, a disparate decanuclear nickel cluster was isolated. Its nickel metal core features a pudgy tetrahedron, surrounded by four apical H_3thmmg^{2-} ligands and 8 mat$^-$ ligands on the six sides of the tetrahedron. Furthermore, the magnetic properties of **Ni_8** and **Ni_{10}** clusters were investigated.

The synthetic routes of the **Ni_8** and **Ni_{10}** clusters are displayed in Scheme S1 (Supporting information). Reaction of $Ni(NO_3)_2{\cdot}6H_2O$, H_5thmmg ligand, $N(CH_2CH_2O)_3$ and Et_3N in EtOH solution under solvothermal condition produces green cubic crystals (**Ni_8**). The **Ni_{10}** cluster has exactly the same synthetic condition except that a new 2-mercapto-5-amino-1,3,4-thiadiazole (Hmat) ligand was added. The thiadiazole ligands have testified to be a good class of ligands for the construction of transition metal clusters, such as Co_{20} [48], Ni_{20} [49], Ni_9 [50], Ag_{11} [51], so Hmat is dominant auxiliary ligand to construct various Ni clusters. As expected, the Hmat participates in coordination in **Ni_{10}** cluster. In addition, the hydroxide is an ideal building-component for high-nuclearity metal clusters. Here, the triethylamine was added to adjust the alkaline condition generating more OH^- to construct high-nuclearity Ni clusters. Triethanolamine as an auxiliary ligand was added in the syntheses of **Ni_8** and **Ni_{10}**, whereas it was not embedded into the final structures. But it is essential for the formation of crystalline products of **Ni_8** and **Ni_{10}**, because no crystals dissolved out when triethanolamine was removed.

The X-ray crystallographic analysis indicates **Ni_8** belongs to monoclinic space group *C*2/*c* and the asymmetric unit contains half of a **Ni_8** molecular cluster and one NO_3^-. As shown in Fig. 1a, the total **Ni_8** cluster is a cationic cluster with molecular formula $[Ni_8O(H_3thmmg)_6]^{2+}$ and two free NO_3^- counter anions. The **Ni_8** skeleton is comprised of 8 Ni^{2+}, 1 O^{2-} and 6 H_3thmmg^{2-} ligands and the Ni/O core is two centrosymmetric cubanes linked by sharing an O^{2-} ion (Fig. 1c). All Ni^{2+} ions are six-coordinated distorted octahedral geometry with N atoms and different O atoms from H_3thmmg^{2-} ligands and an O^{2-} ion (Fig. 1b). Ni1, Ni3 and Ni4 coordinate with 2 COO^-, 2 OH^-, 1 NH^- and 1 O^{2-}, and Ni2 is linked by 6 OH^- from three H_3thmmg^{2-} ligands. The ranges of Ni-O and Ni-N bonds are 2.008-2.1735 Å and 2.120-2.126 Å. The O-Ni-O and O-Ni-N angles fall into the range of 83.40°-172.93° and 80.52°-163.06°. The H_3thmmg^{2-} ligand adopts only one μ_7-η^1:η^1:η^2:η^3 chelating-bridging coordination mode (Fig. S1a in Supporting information) in the periphery to stabilize the core of **Ni_8** cluster. One O^{2-} ion in the center of **Ni_8** generated in situ plays an important effect on the assembly of **Ni_8** cluster, which bridges six Ni^{2+} ions forming a typical octahedron (Fig. 1d) with Ni···Ni distances in the range of 3.037-3.074 Å.

As shown in Figs. 1e and f, the discrete **Ni_8** molecular clusters stack to a 3D network structure by hydrogen-bond interactions formed by H_3thmmg^{2-} ligand and free NO_3^- (Table S1 in Supporting information). NH^- is hydrogen-bonded to free OH^- of H_3thmmg^{2-} ligands with N···O distances for 2.932 and 2.836 Å and N···H-O angles for 156.06° and 159.88°. The NO_3^- counter anion makes a great contribution to the formation of supramolecular interactions, in which all three O atoms are as the acceptors of three coordinated OH^- of H_3thmmg^{2-} ligands with O···O contacts at 2.608, 2.652 and 2.709 Å and O···H-O angles at 154.5°, 174.9° and 160.01°. Besides, the COO^- can be as the acceptor of OH^- of H_3thmmg^{2-} and forms the hydrogen bonds (O···O distances: 2.676, 2.706 and 2.780 Å; O···H-O angles: 173.04°, 165.69° and 159.29°).

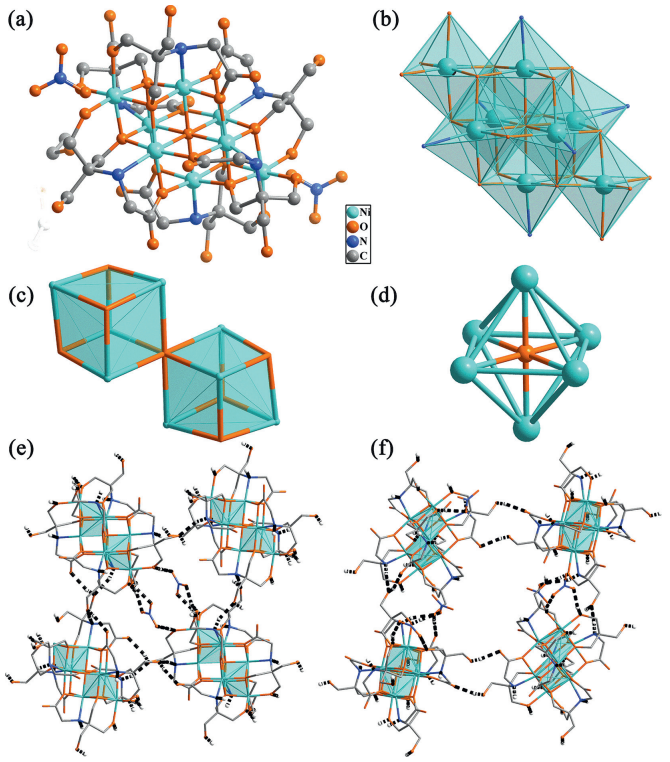

Fig. 1. (a) The total molecular structure of **Ni_8** cluster. (b) The coordination modes of all Ni^{2+} ions of the **Ni_8** cluster. (c) The bi-cubane Ni_8O_8 core. (d) The coordinated Ni_6 octahedron with one O^{2-} ions in the center. (e) and (f) The molecule packing and hydrogen bond interactions of **Ni_8** at different directions.

When a new 2-mercapto-5-amino-1,3,4-thiadiazole (Hmat) ligand was added into the synthesis condition of **Ni_8**, a new ten-nuclearity Ni cluster was isolated. It crystallizes in triclinic *P*-1 space group and the asymmetric unit contains an intact **Ni_{10}** cluster molecule comprised of 10 Ni^{2+} ions, 1 O^{2-}, 2 OH^-, 4 H_3thmmg^{2-} and 8 mat$^-$ (Fig. 2a). The **Ni_{10}** metal skeleton looks like a pudgy tetrahedron (Fig. 2b). Its four vertexes are four Ni^{2+} ions and the remanent six Ni^{2+} ions are located in the tetrahedral cavity in which four Ni^{2+} ions form a Ni_4 square connecting with the other branched 2 Ni^{2+} ions on opposite sides of the square by OH^- and mat$^-$ ligands. A O^{2-} ion is trapped into the center of the Ni_4 square adopting a m_4 coordination mode with the Ni-O distances in the range of 2.132(4)-2.197(4) Å. Obviously, the total **Ni_{10}** metal skeleton is protected by one O^{2-} in the middle of Ni_4 square, two OH^-, 4 H_3thmmg^{2-} and 8 mat$^-$ ligands. Two OH^- connect the middle Ni_4 square and the other two nickel ions in the tetrahedral cavity. Four H_3thmmg^{2-} ligands are located at the four vertices of the tetrahedron, coordinating with the four nickel ions at the vertices (Fig. 2c). 8 mat$^-$ ligands are all on the six sides of the tetrahedron, in which four mat$^-$ ligands are attached on the four sides with approximately equal length and the remaining a longer and a shorter side fix two mat$^-$ ligands in the both sides (Fig. 2d).

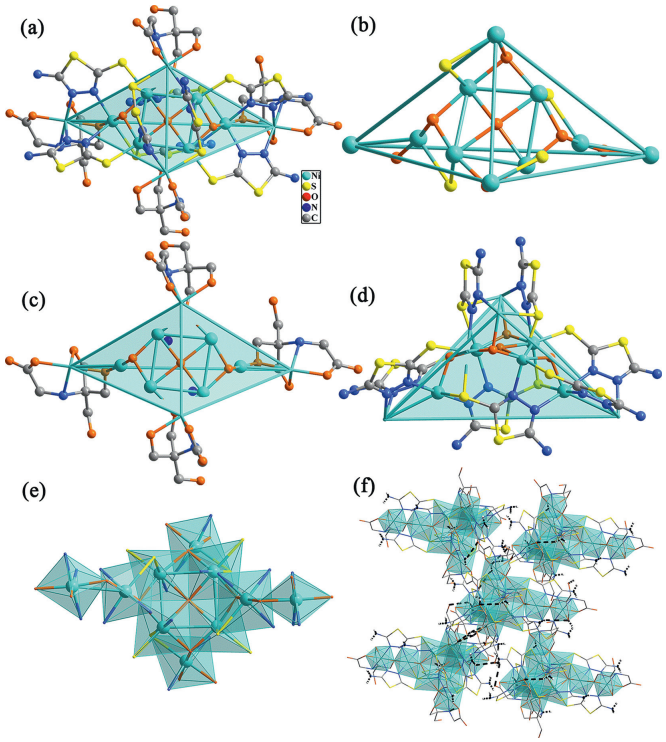

Fig. 2. (a) The molecular structure of **Ni_{10}** cluster. (b) The tetrahedral $Ni_{10}O_7S_4$ core. (c, d) The coordination positions of H_3thmmg^{2-} and mat^- ligands in the **Ni_{10}** cluster. (e) The six-coordinated distorted octahedral geometry of all Ni^{2+} ions in the **Ni_{10}** cluster. (f) The hydrogen bond interactions of **Ni_{10}**.

Same as the **Ni_8** cluster, all Ni^{2+} ions adopt six-coordinated distorted octahedral geometry with N, S and O atoms (Fig. 2e). Four Ni^{2+} ions of the intermediate square are combined by three O atoms (1 O^{2-}, 1 OH^- and 1 $OH^-H_3thmmg^{2-}$), two sulfydryl from two mat^- ligands and one N atom of mat^- ligand. Two branched Ni^{2+} ions on opposite sides of the square in the tetrahedral cavity have a same NiO_2N_3S coordination mode with 1 OH^-, 1 H_3thmmg^{2-} and 4 mat^- ligands. Four vertical Ni^{2+} ions of the tetrahedron have two kinds of coordination modes, NiO_3N_3 from one H_3thmmg^{2-} and 2 mat^- ligands and NiO_3N_2S from 1 H_3thmmg^{2-} and 2 mat^- ligands. Besides, four H_3thmmg^{2-} ligands have two kinds of connection modes, namely, μ_5-η^1:η^1:η^1:η^2 and μ_6-η^1:η^1:η^1:η^3 (Figs. S1b and c in Supporting information). The mat^- ligands have μ_3-η^1:η^1:η^1 and μ_4-η^1:η^1:η^2 connection modes (Figs. S1e and f in Supporting information).

Similarly, the three-dimensional supramolecular structure of the **Ni_{10}** cluster is self-assembly driven by hydrogen-bond interactions deriving from the free $-NH_2$ of mat^- ligands, OH^- and COO^- of H_3thmmg^{2-} (Fig. 2f and Table S2 in Supporting information). Every $-NH_2$ of eight mat^- ligands is involved in the formation of the hydrogen-bond network, in which six COO^- and two OH^- of H_3thmmg^{2-} are as the acceptors to form N-H···O interactions (N···O lengths: 2.723-3.033 Å; N-H···O angles: 121.72°-166.24°). Moreover, two coordinated OH^- of two H_3thmmg^{2-} are hydrogen-bonded to two COO^- of two H_3thmmg^{2-} from another two **Ni_{10}** cluster molecules and O···O contacts are at 2.610 and 2.565 Å, while O···H-O angles are at 155.67° and 139.45°. The above hydrogen-bond interactions make each **Ni_{10}** molecule linked with the adjacent another four cluster molecules, stretching to form a supramolecular structure.

Fourier transform infrared (FT-IR) spectra of **Ni_8** and **Ni_{10}** were measured in the range of 4000-500 cm^{-1}. Combined with Fig. S4a (Supporting information) and the analysis of the knowledge

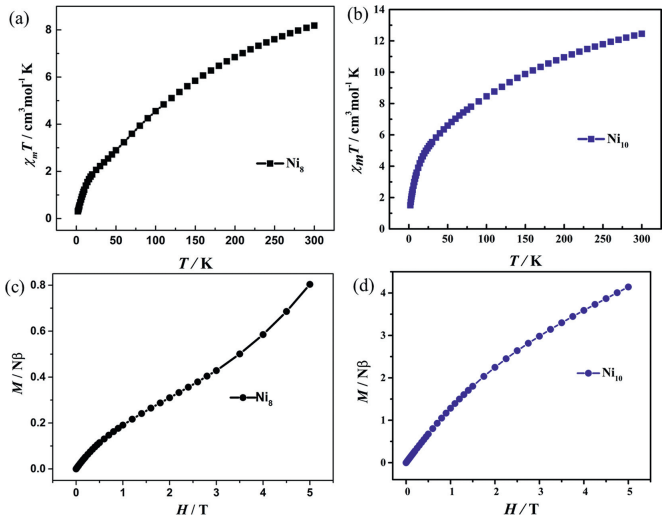

Fig. 3. (a, b) Temperature dependence of $\chi_m T$ measured under a 1000 Oe dc field for **Ni_8** and **Ni_{10}**. (c, d) Field dependence of the magnetizations measured at 2 K for **Ni_8** and **Ni_{10}**.

learned, it is concluded that the broadband absorptions at 3405 cm^{-1} and 3272 cm^{-1} are the stretching vibrations of N-H and O-H from the H_5thmmg ligand. And the absorption peaks at 2930 cm^{-1} and 2865 cm^{-1} are corresponding to the intramolecular saturated C-H stretch. The bending vibration of the C=O and C-O from $-COO^-$ are at 1625 cm^{-1} and 1024 cm^{-1}. The bending vibration of saturated C-H bond is at 1384 cm^{-1}. FT-IR spectrum of **Ni_{10}** is similar to that of **Ni_8**, except for the addition of C=N bending vibration from Hmat ligand at 1530 cm^{-1} and the adsorption of CO_2 from air at 2360 cm^{-1} (Fig. S4b in Supporting information). The thermogravimetries of **Ni_8** and **Ni_{10}** were studied by dry solid samples under N_2 atmosphere from 30 °C to 800 °C. As shown in Fig. S6a (Supporting information), the **Ni_8** and **Ni_{10}** display the weight loss in 30-90 °C and 30-110 °C respectively, corresponding to the loss of ethanol molecules. The skeletons of **Ni_8** and **Ni_{10}** remain stable to 290 °C and 240 °C. Subsequently, the obvious weight loss could be found owing to the collapse of the frameworks.

To explore the magnetic exchange coupling of **Ni_8** and **Ni_{10}** clusters, direct current (dc) magnetic susceptibility was measured under a 1000 Oe dc magnetic field (Fig. 3). As shown in Figs. 3a and b, the experimental $\chi_m T$ values for **Ni_8** and **Ni_{10}** are 8.18 and 12.45 cm^3 K/mol at 300 K, which is approximate to the calculated values for 8 and 10 magnetically isolated Ni(II) centers (9.68 cm^3 K/mol for **Ni_8**; 12.1 cm^3 K/mol for **Ni_{10}**, with S = 1 and g = 2.2 per Ni(II) ion) [52]. During cooling from 300–25 K, the $\chi_m T$ of **Ni_8** and **Ni_{10}** slightly decrease and the values correspondingly reach 2.06 and 5.13 cm^3 K/mol at 25 K. Further decreasing the temperature to 2 K, for **Ni_8** and **Ni_{10}**, the $\chi_m T$ values rapidly decrease to minimum 0.30 and 1.51 cm^3/mol, which attributes to the stronger intramolecular antiferromagnetic interactions at low temperatures [53–55]. Furthermore, the χ_m^{-1} *vs.* *T* plots can be fitted with the Curie–Weiss law in the range of 60–300 K for **Ni_8** and 55–300 K for **Ni_{10}** (Figs. S2a and b in Supporting information), giving C = 13.58 mol/cm^3; $\theta = -196.91$ K (**Ni_8**) and C = 15.54 mol/cm^3; $\theta = -80.77$ K (**Ni_{10}**). The negative Weiss constants θ of **Ni_8** and **Ni_{10}** further confirm their antiferromagnetic interactions [56].

The field-dependent magnetization characterizations of **Ni_8** and **Ni_{10}** were recorded in the range of 0-5 T at 2 K to investigate the nature of the metamagnetism [57]. As shown in Figs. 3c and d, the plots of M *vs.* H for **Ni_8** and **Ni_{10}** exhibit the magnetization values gradually decrease at low field. The maximum magnetization values of **Ni_8** and **Ni_{10}** at 5 T are 0.80 and 4.14 Nβ much lower than

the corresponding theoretical value 17.6 and 22.0 Nβ, also suggesting their antiferromagnetic interactions.

The temperature-dependent alternating current (ac) magnetic susceptibilities under $H_{dc} = 0$ Oe for **Ni$_8$** and **Ni$_{10}$** were measured at 500 and 1000 Hz. Demonstrably, no frequency dependent signals for in- and out-of-phase were observed (Figs. S3a and b in Supporting information), indicating no single-molecule magnet behaviors (SMMs).

In conclusion, by using the H_5thmmg ligand under solvothermal condition, an 8-nuclear Ni cluster was isolated. And when the Hmat ligand was introduced into the synthesis of the **Ni$_8$**, a 10-nuclear Ni cluster assembled by H_3thmmg^{2-} and mat$^-$ mixed ligands was obtained. The above results demonstrate the amino acid-derived H_5thmmg ligand is an effective ligand for constructing polymetallic clusters. The **Ni$_8$** cluster has a cationic metallic skeleton built by two centrosymmetric cubanes $Ni_4(\mu_3\text{-}O)_3(\mu_6\text{-}O)$ linked by sharing an O^{2-} ion and the periphery is protected by six H_3thmmg^{2-} ligands. The metal core of **Ni$_{10}$** cluster is a pudgy tetrahedron, whose four vertexes are four Ni^{2+} ions and the remanent six Ni^{2+} ions are located in the tetrahedral cavity. Four H_3thmmg^{2-} ligands are located at the four vertices of the tetrahedron and 8 mat$^-$ ligands are all on the six sides of the tetrahedron. In addition, complexes **Ni$_8$** and **Ni$_{10}$** display the antiferromagnetic interactions.

Declaration of competing interest

The authors declare that they have no known competing financial interests or personal relationships that could have appeared to influence the work reported in this paper.

Acknowledgments

We would like to gratefully acknowledge financial support from the National Natural Science Foundation of China (Nos. 22101148, 22071126) and the Natural Science Foundation of Shandong Province (No. ZR2021QB008).

Supplementary materials

Supplementary material associated with this article can be found, in the online version, at doi:10.1016/j.cclet.2022.03.113.

References

[1] J. Yan, B.K. Teo, N. Zheng, Acc. Chem. Res. 51 (2018) 3084–3093.
[2] X. Zhao, S.Q. Zang, X. Chen, Chem. Soc. Rev. 49 (2020) 2481–2503.
[3] J. Yang, R. Jin, J. Phys. Chem. C 125 (2021) 2619–2625.
[4] P. Zhang, Y.N. Guo, J. Tang, Coord. Chem. Rev. 257 (2013) 1728–1763.
[5] I. Chakraborty, T. Pradeep, Chem. Rev. 117 (2017) 8208–8271.
[6] R. Jin, C. Zeng, M. Zhou, Y. Chen, Chem. Rev. 116 (2016) 10346–10413.
[7] Z. Wang, R.K. Gupta, G.G. Luo, D. Sun, Chem. Rec. 20 (2020) 389–402.
[8] S.S. Zhang, X.C. Zhang, L. Feng, et al., Sci. China Chem. 64 (2021) 2118–2164.
[9] Y.M. Su, Z. Wang, S.S. Zhang, et al., Sci. China Chem. 64 (2021) 1482–1486.
[10] Z. Wang, H.F. Su, P. Huang, et al., Sci. China Chem. 63 (2019) 16–20.
[11] A. Muller, P. Gouzerh, Chem. Soc. Rev. 41 (2012) 7431–7463.
[12] S.T. Zheng, G.Y. Yang, Chem. Soc. Rev. 41 (2012) 7623–7646.
[13] J. Kobylarczyk, E. Kuzniak, M. Liberka, et al., Coord. Chem. Rev. 419 (2020) 213394.
[14] Y.Z. Zheng, G.J. Zhou, Z. Zheng, R.E.P. Winpenny, Chem. Soc. Rev. 43 (2014) 1462–1475.
[15] X.Y. Zheng, J. Xie, X.J. Kong, L.S. Long, L.S. Zheng, Coord. Chem. Rev. 378 (2019) 222–236.
[16] J.L. Liu, Y.C. Chen, F.S. Guo, M.L. Tong, Coord. Chem. Rev. 281 (2014) 26–49.
[17] X.Y. Zheng, X.J. Kong, Z. Zheng, L.S. Long, L.S. Zheng, Acc. Chem. Res. 51 (2018) 517–525.
[18] W.H. Fang, L. Zhang, J. Zhang, Chem. Soc. Rev. 47 (2018) 404–421.
[19] C. Papatriantafyllopoulou, E.E. Moushi, G. Christou, A.J. Tasiopoulos, Chem. Soc. Rev. 45 (2016) 1597–1628.
[20] K. Liu, W. Shi, P. Cheng, Coord. Chem. Rev. 289-290 (2015) 74–122.
[21] X. Yang, R.A. Jones, S. Huang, Coord. Chem. Rev. 273-274 (2014) 63–75.
[22] A. Caneschi, D. Gatteschi, R. Sessoli, et al., J. Am. Chem. Soc. 113 (1991) 5873–5874.
[23] A.J. Tasiopoulos, A. Vinslava, W. Wernsdorfer, K.A. Abboud, G. Christou, Angew. Chem. Int. Ed. 43 (2004) 2117–2121.
[24] M. Manoli, S. Alexandrou, L. Pham, et al., Angew. Chem. Int. Ed. 55 (2016) 679–684.
[25] M. Soler, W. Wernsdorfer, K. Folting, M. Pink, G. Christou, J. Am. Chem. Soc. 126 (2004) 2156–2165.
[26] T.C. Stamatatos, K.A. Abboud, W. Wernsdorfer, G. Christou, Angew. Chem. Int. Ed. 47 (2008) 6694–6698.
[27] Z.J. Zhong, H. Seino, Y. Mizobe, et al., J. Am. Chem. Soc. 122 (2000) 2952–2953.
[28] C.J. Milios, R. Inglis, A. Vinslava, et al., J. Am. Chem. Soc. 129 (2007) 12505–12511.
[29] J.C. Goodwin, R. Sessoli, D. Gatteschi, et al., Dalton Trans. (2000) 1835–1840.
[30] A.M. Ako, V. Mereacre, Y. Lan, et al., Inorg. Chem. 49 (2010) 1–3.
[31] A. Cornia, A.C. Fabretti, P. Garrisi, et al., Angew. Chem. Int. Ed. 43 (2004) 1136–1139.
[32] J.W. Sharples, D. Collison, Coord. Chem. Rev. 260 (2014) 1–20.
[33] S.T. Ochsenbein, M. Murrie, E. Rusanov, et al., Inorg. Chem. 41 (2002) 5133–5140.
[34] E.K. Brechin, S.G. Harris, A. Harrison, et al., Chem. Commun. (1997) 653–654.
[35] R. Boča, Coord. Chem. Rev. 248 (2004) 757–815.
[36] J. Krzystek, A. Ozarowski, J. Telser, Coord. Chem. Rev. 250 (2006) 2308–2324.
[37] S. Wang, X. Gao, X. Hang, et al., J. Am. Chem. Soc. 140 (2018) 6271–6277.
[38] K. Li, Z. Zhuang, W. Chen, W. Liao, Cryst. Growth Des. 20 (2020) 4164–4168.
[39] H. Han, L. Kan, P. Li, et al., Sci. China. Chem. 64 (2021) 426–431.
[40] K. Sheng, B.Q. Ji, L. Feng, et al., New J. Chem. 44 (2020) 7152–7157.
[41] Z. Wang, Z. Jagličić, L.-L. Han, et al., CrystEngComm 18 (2016) 3462–3471.
[42] G. Karotsis, C. Stoumpos, A. Collins, et al., Dalton Trans. (2009) 3388–3390.
[43] T.C. Stamatatos, A. Escuer, K.A. Abboud, et al., Inorg. Chem. 47 (2008) 11825–11838.
[44] A. Perivolaris, C.C. Stoumpos, J. Karpinska, et al., Inorg. Chem. Front. 1 (2014) 487–494.
[45] C.G. Efthymiou, L. Cunha-Silva, S.P. Perlepes, et al., Dalton Trans. 45 (2016) 17409–17419.
[46] M. Murrie, D. Biner, H. Stœckli-Evans, H.U. Güdel, Chem. Commun. (2003) 230–231.
[47] X.Y. Li, Y. Zou, S.D. Han, G.M. Wang, Inorg. Chem. Front. 8 (2021) 4186–4191.
[48] B. Mu, Q. Wang, R.D. Huang, RSC Adv. 6 (2016) 12114–12122.
[49] L. Dong, R. Huang, Y. Wei, W. Chu, Inorg. Chem. 48 (2009) 7528–7530.
[50] J.Y. Liu, Z.Y. Liu, L.J. Zhang, et al., CrystEngComm 15 (2013) 6413–6423.
[51] X.Y. Li, H.F. Su, J. Xu, Inorg. Chem. Front. 6 (2019) 3539–3544.
[52] G. Aromi, S. Parsons, W. Wernsdorfer, E.K. Brechin, E.J. McInnes, Chem. Commun. (2005) 5038–5040.
[53] F. Luo, J.M. Zheng, M. Kurmoo, Inorg. Chem. 46 (2007) 8448–8450.
[54] Y. Chen, Z.W. Guo, Y.P. Chen, et al., Inorg. Chem. Front. 8 (2021) 1303–1311.
[55] Y. Chen, Z.W. Guo, X.X. Li, S.T. Zheng, G.Y. Yang, CCS Chem. (2021) 1232–1241.
[56] X.Y. Li, H.F. Su, Q.W. Li, et al., Angew. Chem. Int. Ed. 58 (2019) 10184–10188.
[57] Y.J. Ma, S.D. Han, Y. Mu, et al., Cryst. Growth Des. 18 (2018) 3477–3483.